

# A new technique to measure loss, effective refractive index and electric field distribution of THz porous fibers

S. Atakaramians<sup>1,2</sup>, S. Afshar V.<sup>2</sup>, M. Nagel<sup>3</sup>, T. M. Monro<sup>2</sup>, and D. Abbott<sup>1</sup>

<sup>1</sup> Adelaide T-ray Group, School of Electrical & Electronic Engineering, The University of Adelaide, Australia

<sup>2</sup> Institute for Photonics & Advanced Sensing, School of Chemistry & Physics, The University of Adelaide, Australia

<sup>3</sup> Institut für Halbleitertechnik, RWTH Aachen University, Germany

shaghik@eleceng.adelaide.edu.au

**Abstract:** We developed a new technique, employing a probe-tip, to measure both  $\alpha_{\text{eff}}$  and  $n_{\text{eff}}$  of porous fibers. Moreover, using this approach, we measure the evanescent electric field as a function of frequency.

**OCIS codes:** (260.3090) Infrared, far; (230.7370) Waveguides; (300.6495) Spectroscopy, terahertz;

## 1. Introduction

THz porous fibers have been identified as a means of achieving low losses, low dispersion and high birefringence among terahertz polymer fibers [1-6]. Porous fibers are air-clad fibers with sub-wavelength features in the core. Compared with solid-core air-clad fibers with sub-wavelength dimensions [7,8], referred to as microwires, porous fibers offer improved confinement and lower dispersion and can be designed to maintain the polarization of the field by using asymmetrical sub-wavelength air holes [3,4]. The low-dispersion characteristics of these porous fibers compared with their microwire counterparts and the birefringence characteristics have experimentally been confirmed [4]. Losses as low as  $0.01\text{cm}^{-1}$  [5] and  $0.02\text{cm}^{-1}$  [6] have also been reported for porous fibers. In the former report, a secondary fiber was located to and translated along the fiber being characterized in order to decouple the pulse and measure it using a bolometer, while in the later a standard THz time domain spectroscopy system with photoconductive antennae was used. Here, we propose a new technique in which we use a micromachined photoconductive probe-tip directly to measure the THz electric field at the vicinity of the fiber surface and hence measure simultaneously both the absorption coefficient ( $\alpha_{\text{eff}}$ ) and effective refractive index ( $n_{\text{eff}}$ ) of the propagating mode of a fiber. Moreover, this approach enables us, for the first time to the best of our knowledge, to accurately study the radial distribution of evanescent field in the air-clad of these fibers as a function of frequency. We present the experimental results and demonstrate a good agreement with the numerical results based on structural information obtained from SEM images of the real fibers and under assumption of no field distortion by the probe.

## 2. Results

A mode-locked Ti:sapphire laser with a pulse width of less than 100 fs, central frequency of 800 nm and a repetition rate of 80 MHz is used to drive the emitter and detector. An antenna array [9] consisting of 10 antenna elements on a 1.7 mm thick silica substrate is used for generation of THz pulses, while a probe-tip, Fig. 1(d), a photoconductive switch with a pair of tapered electrodes on a triangular-shaped LT-GaAs substrate [10] is utilized for sampling of THz pulses. The probe-tip allows sampling of the THz pulses along the waveguide. This is possible because the evanescent field of the mode propagating along the porous fiber expands into the air-clad region. Therefore, instead of measuring three different fibers, the approach employed in [4], or the cut-back method, the propagating mode is directly sampled at three different positions along the waveguide. This eliminates the uncertainty that usually exists in the loss measurement due to the quality and repeatability of the cleaved end-face of the porous fibers [4].

The schematic of the experimental set-up is shown in Fig. 1(a). In order to increase the coupling efficiency of THz pulses into the fiber and block the stray beams a metallic cone with an 800  $\mu\text{m}$  pin-hole at vertex is employed. The waveguide is mounted on two specially designed fiber holders at two ends and is kept straight. This minimizes the losses due to the curvature of the fiber (bend loss). A 540  $\mu\text{m}$  diameter cyclic-olefin copolymer (COC) porous fiber, Fig. 1(b), is characterized. Two cameras are employed to monitor the alignment of the probe-tip and waveguide, Fig. 1(c). The emitter, focusing optical lens, and waveguide are situated on a sliding table and the detector is fixed, Fig. 1(a). The moving plate is slid to the left and three positions with 50 mm separations are sampled. For every position, the signal without the waveguide has also been measured and used as reference to evaluate the noise level. Figs. 2(a) & (b) show the measured  $\alpha_{\text{eff}}$  and  $n_{\text{eff}}$  values. The results are only illustrated within the range, which is above the noise level (black vertical dotted lines). The theoretical  $\alpha_{\text{eff}}$  and  $n_{\text{eff}}$  values of a *real* porous fiber (simulation conducted based on SEM image of the fiber Fig. 1(b)) are also depicted with red dashed lines. The vertical error bars represent the standard variations due to fiber length and signal variation. Losses as low as  $0.01\text{cm}^{-1}$  are measured and the  $n_{\text{eff}}$  curve follows closely the expected low dispersion theoretical values.

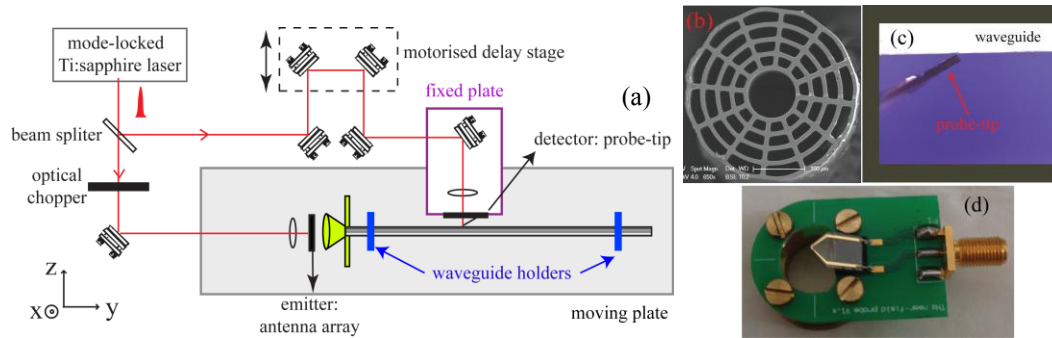


Fig. 1. (a) Schematic of experimental setup, (b) Porous fiber cross-section, (c) Monitoring probe-tip and fiber distance, and (d) Probe-tip.

We have also measured the frequency-dependent radial field distribution of a 600  $\mu\text{m}$  diameter COC porous fiber. For this purpose, the probe-tip was shifted away from the fiber and the THz pulses are measured at different radial positions. Fig. 2(c) shows the measured radial electric field distribution at 0.23 & 0.28 THz. The fields are normalized to the respective maximum amplitude at the porous fiber surface. The curves indicate that increasing the frequency increases the confinement of the field to the fiber, as expected. For comparison, the theoretical values of the normalized radial distribution of the electric fields of a 600  $\mu\text{m}$  diameter *real* porous fiber are calculated and shown with solid lines.

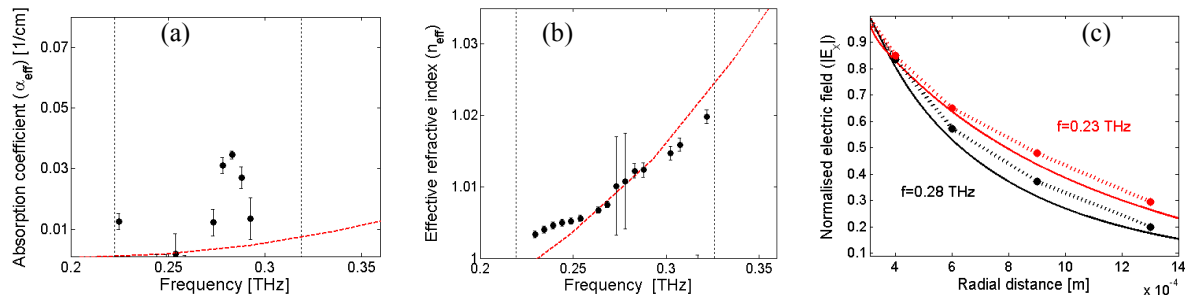


Fig. 2. (a)  $\alpha_{\text{eff}}$  & (b)  $n_{\text{eff}}$  of a 540  $\mu\text{m}$  diameter porous fiber. (c) Frequency dependent radial field distribution of a 600  $\mu\text{m}$  diameter porous fiber. Dots represent experimental values, while solid and dashed lines represent the theoretically values based on the SEM image of the porous fiber.

### 3. Conclusion

Here, we present a novel approach for measuring loss and dispersion of porous fibers. The THz pulses are sampled along the fiber without any need for cut-back measurement. Moreover, we measure the evanescent field of the propagating mode by exploiting the probe-tip. Further detail of our measurement will be presented at the conference.

**4. Acknowledgment:** We gratefully acknowledge A/Prof Ole Bang from Technical University of Denmark for supplying the COC billet.

### 5. References

- [1] A. Hassani, A. Dupuis, and M. Skorobogatiy, "Low loss porous terahertz fibers containing multiple subwavelength holes," *Appl. Phys. Lett.*, **92**, 071101 (2008).
- [2] S. Atakaramians, S. Afshar V., B. M. Fischer, D. Abbott, and T. M. Monro, "Porous fibers: A novel approach to low loss THz waveguides," *Opt. Express*, **16**, 8845–8854 (2008).
- [3] S. Atakaramians, S. Afshar, B. M. Fischer, D. Abbott, and T. M. Monro, "Low loss, low dispersion and highly birefringent terahertz porous fibers," *Opt. Commun.*, **282**, 36–38 (2008).
- [4] S. Atakaramians, S. Afshar V., M. Nagel, H. Ebendorff-Heidepriem, B. M. Fischer, D. Abbott, and T. M. Monro, "THz porous fibers: Design, fabrication and experimental characterization," *Opt. Express*, **17**, 14 053–14 062 (2009).
- [5] A. Dupuis, J.-F. Allard, D. Morris, K. Stoeffler, C. Dubois, and M. Skorobogatiy, "Fabrication and THz loss measurements of porous subwavelength fibers using a directional coupler method," *Opt. Express*, **17**, 8012–8028 (2009).
- [6] A. Dupuis, A. Mazhorova, F. Désévéday, M. Rozé, and M. Skorobogatiy, "Spectral characterization of porous dielectric subwavelength THz fibers fabricated using a microstructured molding technique," *Opt. Express*, **18**, 13813–13828 (2010).
- [7] L.J. Chen, H.W. Chen, T.F. Kao, J.Y. Lu and C.K. Sun, "Low-loss subwavelength plastic fiber for terahertz waveguiding," *Opt. Lett.*, **33**, 308–310 (2006).
- [8] S. Atakaramians, S. Afshar V., H. Ebendorff-Heidepriem, B. M. Fischer, T. Monro and D. Abbott, "Low loss terahertz transmission," *Proc. SPIE, Smart Materials, Nano- and Micro-Smart Systems*, Vol. **6414**, Adelaide, Australia, Art. No. 64140I (2006).
- [9] D. Saeedkia, R. R. Mansour and S. Safavi-Naeini-S, "Analysis and design of a continuous-wave terahertz photoconductive photomixer array source," *IEEE Trans. on Antennas and Propagation*, **53**, 4044–4050 (2005).
- [10] M. Wächter, M. Nagel, and H. Kurz, "Tapered photoconductive terahertz field probe tip with subwavelength spatial resolution," *Applied Physics Letters*, **95**, 041112 (2009).